A Recovery Performance Study of Compressive Sensing Methods on Antenna Array Diagnosis from Near-Field Measurements

Oluwole John Famoriji and Thokozani Shongwe

Department of Electrical and Electronic Engineering Science
University of Johannesburg, P.O. Box 524, Auckland Park, 2006, Johannesburg, South Africa
famoriji@mail.ustc.edu.cn, tshongwe@uj.ac.za

Abstract **─** Antenna testing consists locating the potential defaults from radiated field measurements. It has been established in literature, that compressive sensing methods provide faster results in failure detection from smaller number of measurement data compared to the traditional back-propagation mechanisms. Compressive sensing (CS) methods require a priori measurement of failure-free reference array and require small number of measurements for diagnosis. However, there are conflicting reports in literature regarding the choice of appropriate CS method, and there is no sufficient comparison study to justify which one is a better choice under a very harsh condition. In this study, recovery performance test of CS methods for the diagnosis of antenna array from few near-field measured data under various signal-to-noise ratios (SNRs) is presented. Specifically, we tested three prominent regularization procedures: total variation (TV), mixed $\mathrm{l}_1/\mathrm{l}_2$ norm, and minimization of the l_1 in solving diagnosis problems in antenna array. Linear system that relates the difference between near-field measured data from reference antenna (RA) array and array under test (AUT), and the difference that exist between coefficients of RA and the AUT, is solved by the three compressive sensing regularization methods. Numerical experiment of a 10×10 rectangular waveguide array under realistic noise scenario, operating at 10 GHz is used to conduct the test. Minimization l_1 technique is more robust to additive data noise. It exhibits better diagnosis at 20 dB and 10 dB SNR, making it a better candidate for noisy measured data as compared to other techniques.

Index Terms **─** Antenna array diagnosis, antenna testing, compressive sensing, near-field, low SNR.

I. INTRODUCTION

Nowadays, near-field equipment is used for routine array test. Apart from radiation pattern measurements, diagnosis of antenna array is another major application. Current and future technologies employ sophisticated active or phased arrays with large elements. For example, large array employed in RADAR systems, full MIMO systems, massive MIMO, and personal communication devices that require complex antenna arrays. As a result, there will always be a demand for fast and accurate complex antenna systems diagnosis, to resolve the unacceptable radiation pattern distortion caused by element (s) failure in the array.

Many antenna array diagnosis methods, based on genetic algorithms [1], [2], exhaustive search [3], matrix inversion [4], and MUSIC [5], have been developed in literature to identify faulty antenna elements in an array. All the methods compare the array under test (AUT) with the radiation pattern of an "error free" reference array. All the methods in [1-5] need big measurement samples for large antenna arrays, to get reliable diagnosis. Reducing the measurement samples, compressive sensing (CS) based techniques have been reported in [6]-[9]. Despite the compelling outcome, the methods in [1]-[9] focused on the detection of sparsity pattern of a failed array, i.e., failed elements location, not on the complex blockage, as addressed in [10]. Recently, compressive sensing approaches have shown great advantages in terms of reduced number of measurement data, reconstruction accuracy, and simulation time [11]. Compressive sensing (CS) is a method of signal processing through which it is possible to reconstruct or recover a signal from a set of linear measurements rather than the original signal itself, and the measurements set is less than the signal. Consequently, the primary signal will be reconstructed from measurement matrix, which is ill-posed as a result of decreased dimension.

In literatures, such as [7-11], differential scenario with sparse recovery algorithms have been used to diagnose antenna arrays and retrieve element excitations. This method results to a small number of unknown, however, they require a well detailed array model with the exact information of the radiation patterns of the antenna to generate appropriate results. Particularly, total variation (TV) norm, mixed ℓ_1/ℓ_2 norm and minimization of the ℓ_1 norm were tested to proffer solution to an inversion issue. However, based on the acquired information, no work has thoroughly compared the methods, particularly the recovery performance

Submitted On: June 15, 2018
Accepted On: June 10, 2021
https://doi.org/10.47037/2021.ACES.J.360805
1054-4887 © ACES

under different signal-to-noise ratios (SNRs). For a noisy measured data, which of those methods is more suitable? i.e., which method gives better recovery performance for near-field measured data with low SNR? This paper provides answer to this question. In addition, there are contradicting reports and recommendations in literature. For instance, Fuchs *et al.* [11] recommended the use of mixed ℓ_1/ℓ_2 norm while Migliore [7] recommended minimization of the ℓ_1 norm. Again, these are conflicting results necessitating the further study.

In CS mechanisms, the number of measurements required increases logarithmically and slowly based on the number of unknowns [12-17]. Hence, field synthesis scheme benefits more in sparse recovery-based methods [11]. Modeled diagnostic issues can be evaluated by using the available customs whose calculation times are little more than the standard approaches. Therefore, it is good to show that total time required in getting the array of antenna diagnosed majorly depend on time taken in measurement, with post-processing time of higher magnitude faster. That is the reason that sparse recovery methods with few numbers of measurements will provide faster antenna array diagnosis. Researchers have proposed various compressive sensing algorithms [11], [12]-, [25] but only three of them are reported in this paper because of their robustness and efficiency [4]. Total variation (TV) norm, mixed ℓ_1/ℓ_2 norm and minimization of the ℓ_1 norm methods are adapted and applied to a simulated near-field data of a 10 GHz waveguide array with 100 elements in which failures had been added intentionally. And the recovery performance under low SNR was evaluated, to determine the best algorithm fit for such scenario.

CS methods provide good, reliable, and accurate antenna array diagnosis at low SNR compared to the conventional methods. This is a useful feature, particularly in very harsh measurement environment. Nevertheless, no work has thoroughly compared the CS methods. Furthermore, in a very harsh measurement environment (i.e., low SNR), which of these methods is preferable? That is, which of the methods provide better recovery performance for low SNR near-field measurement? This paper answers this question, specifically; total variation (TV) norm, mixed ℓ_1/ℓ_2 norm and minimization of the ℓ_1 norm were examined to solve an inversion problem. The results obtained will influence the choice of CS diagnosis method especially under very low SNR measurements.

II. DIAGNOSIS PROBLEM OF ANTENNA ARRAY

Here, we consider a rectangular radiating antenna array in space (Fig. 1). The radiated field of antenna is usually considered in phase or/and amplitude within the near-field region. The AUT is as shown in Fig. 1 (b). The associated parameters of AUT is marked with “u” as superscript. Especially, $\boldsymbol{E}^u(x,y)$ is the tangential field that is concentrated on the antenna aperture, i.e.,

$$\boldsymbol{E}^u(x,y) = E_x^u(x,y)\hat{x} + E_y^u(x,y)\hat{y}, \quad (1)$$

where $E_x^u(x,y)\hat{x}$ and $E_y^u(x,y)\hat{y}$ are components x and y of the electric field situated on the aperture Σ respectively. Near-field $N^u(r,\theta,\emptyset)$ is field measured on part of hemispherical surface $(0 \le \theta \le \pi/2, 0 \le \phi \le 2\pi)$ at radius *r* from center of AUT, and $r < 2D^2/\lambda$, D is diameter of the antenna. Also, the near-field of RA is assumed available. The associated parameters are with “o” superscript. $\boldsymbol{E}^o(x,y)$ is the field on RA aperture Σ and $\boldsymbol{N}^o(r,\theta,\emptyset)$ denotes the far-field radiated. For the DA depicted in Fig. 1 (c), the tangential distribution $\boldsymbol{E}(x,y)$ on its aperture equals the difference between the RA and AUT field, and the corresponding near-field $\boldsymbol{N}(r,\theta,\phi)$ is expressed as the difference between the near field of RA and AUT as:

$$\boldsymbol{E}(x,y) = \boldsymbol{E}^u(x,y) - \boldsymbol{E}^o(x,y), \quad (2)$$

$$\boldsymbol{N}(r,\theta,\phi) = \boldsymbol{N}^u(r,\theta,\phi) - \boldsymbol{N}^o(r,\theta,\phi). \quad (3)$$

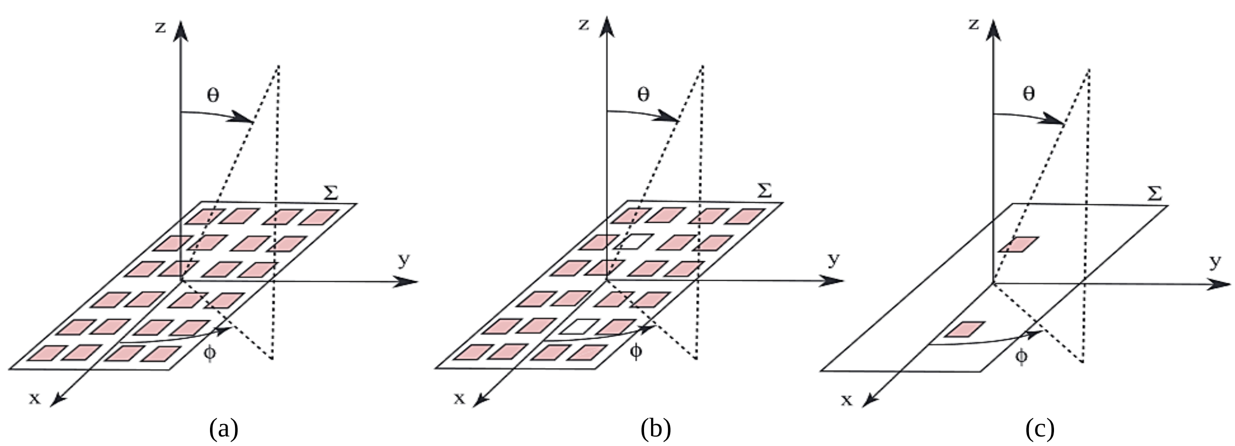

Fig. 1. Antenna array decomposition and modeling for diagnosis. (a) Reference antenna (RA), (b) antenna under test (AUT), and (c) differential antenna (DA). Number of failures here is *2* for 24 elements, and Σ is the aperture [11].

III. COMPRESSED SPARSE RECOVERY TECHNIQUES

The role of matrix inversion technique is to introduce *a priori* knowledge within the inversion. The efficient approach that is required in getting this regularization is by approximately reducing the selected norm q of $\mathbf{x}$ solution. Hence, the optimization problem to be solved becomes:

$$\min_{\mathrm{x}} \|X\|_q \text{ subject to } \|\boldsymbol{y} - \boldsymbol{AX}\|_2 \leq \gamma, \quad (4)$$

where $\|\cdot\|_q$ represents l_q norm, and γ is a function of noise and factors affecting the measurement. Different routines solutions are readily available to solve the convex optimization problem of Eqn. (4), such as [19-25]. The three norms l_q, chosen according to *a priori* knowledge of a differential antenna diagnosis setup, can then be explained for inversion regularization. We can consequently apply them to effectively diagnosis radiating elements.

A. TV norm

According to *a priori* knowledge that solution x has small discontinuities due to the presence of failures. Besides the failures, it is expected that the field x is to be made almost zero. Therefore, TV-norm is a smooth function to regularize x [25]. So, minimizing TV-norm is minimizing its gradient, this is the effect of smoothing. Consider 2-dimensional complex data set $X \in \mathbb{C}^{M \times N}$, TV-norm gives:

$$\|X\|_{TV} = \sum_{m,n} \left|\boldsymbol{X}_{m+1,n} - \boldsymbol{X}_{m,n}\right| + \left|\boldsymbol{X}_{m,n+1} - \boldsymbol{X}_{m,n}\right| \quad (5)$$
$$\|vec(\boldsymbol{\nabla}_x \boldsymbol{X})\|_1 + \left\|vec(\boldsymbol{X}\boldsymbol{\nabla}_y)\right\|_1,$$

vec ($\mathbf{X}$) produces vector *N by M* that has the columns $\mathbf{X}$, stacked beside each other. Gradient matrix $\boldsymbol{\nabla}_x$ and $\boldsymbol{\nabla}_y$ are made up of $M \times M$ and $N \times N$ size, respectively. They are computed as:

$$\boldsymbol{\nabla}_x = \begin{bmatrix} -1 & & 1 & 0 \\ & \ddots & & \ddots \\ 0 & & -1 & 1 \end{bmatrix} \text{ and}$$

$$\boldsymbol{\nabla}_y = \begin{bmatrix} -1 & & 0 \\ 1 & \ddots & \\ & \ddots & -1 \\ 0 & & 1 \end{bmatrix}.$$

Then, the problem of optimization in Eqn. (4) becomes:

$$\min_{\boldsymbol{X}} \|\boldsymbol{X}\|_{TV} \text{ subjects to } \|\boldsymbol{y} - \boldsymbol{A}vec(\boldsymbol{X})\|_2 \leq \epsilon. \quad (6)$$

B. ℓ_1 norm

Since sparse solution X exists, then a search space can be reduced by initiating *a priori* knowledge in inversion. Particularly, the ℓ_1-norm ($\|X\|_1 = \sum_k |x_k|$) is the leading convex surrogate of the appropriate vector estimate. That is, the quasi-norm ℓ_0 that calculates nonzero occurrences of a particular vector). Consequently, ℓ_1 norm technique is an effective method for enhancing the sparse solution [7], [8], [10], [11]. The problem of the regularization is:

$$\min_{X} \|X\|_1 \text{ subject to } \|\boldsymbol{y} - \boldsymbol{A}vec(\boldsymbol{X})\|_2 \leq \epsilon. \quad (7)$$

Minimization of the ℓ_1-norm forces the pointwise sparsity of solution per sample x_k of EM field on the DA aperture.

C. ℓ_1/ℓ_2-norm

The position and dimension of the radiating aperture can be taken. The solution X is grouped into G groups X^g that corresponds to each aperture of the radiating element g. For a faulty element, all regions of discretization x_k^g within the aperture becomes nonzero. Let vector X of dimension *MN* be divided into *G* non-overlapping groups depicted as X^g of size N_g, such as $\sum_{g=1}^{G} N_g = MN$. Then, the mixed ℓ_1/ℓ_2-norm is given as:

$$\|X\|_{1,2} = \sum_{g=1}^{G} \|X^g\|_2 = \sum_{g=1}^{G} \sqrt{\left|x_1^g\right|^2 + \cdots + \left|x_{N_g}^g\right|^2}. \quad (8)$$

Mixed ℓ_1/ℓ_2-norm have similar behavior with ℓ_1 Norm on vector$\|X^1\|_2, \ldots, \|X^g\|_2, \ldots \|X^G\|_2$, it therefore induces group sparsity at the radiating aperture level. The regularized inversion optimization problem is given as:

$$\min_{X} \|X\|_{1,2} \text{ subject to } \|\boldsymbol{y} - \boldsymbol{A}X\|_2 \leq \epsilon. \quad (9)$$

IV. NUMERICAL SIMULATIONS

Considering an open-ended waveguide array constituted by a 10×10 *WR90* waveguides that operates at 10 GHz, aperture size $22.86 \times 10.16\ mm^2$, and spaced uniformly by $\lambda\ and\ \lambda/2$ along x- and y-planes, respectively, as depicted in Figs. 2 (a-c). Because normalized patterns provide sufficient information to obtain substantial results, we considered the normalized pattern as shown in Figs. 2 (d, e). The antenna array's radiation pattern is computed using antenna toolbox in Matlab software. At first, all the elements *N* in the array are excited with the same value in order to emulate RA (i.e., array without failure). To model the AUT, *K* failures in either phase δ_Φ or amplitude δ_A are added.

Practically, noise contaminates measurements; hence, we added a Gaussian noise $\mathbf{n}$ to the radiation pattern of the reference and defaults as $\boldsymbol{y}_n^q = \boldsymbol{y}^q + \boldsymbol{n}^q$ where $q = \{r, d\}$. Noise level is computed by SNR which could be extracted from the highest magnitude of received field to fit with dynamic range of measurement. Then the noise can be given as:

$$n^q = \frac{\mathbb{N}(0,1) + j\mathbb{N}(0,1)}{\sqrt{2}}\, max|\boldsymbol{y}^q|.\, 10^{-SNR_{dB}/20}, \quad (10)$$

where $\mathbb{N}(0,1)$ represents Gaussian random vector with 0 mean and 1 standard deviation. SNR can be varied in random near-field measurements, and subjecting the compressive sensing methods to different scenario can provide recovery performance of each methods.

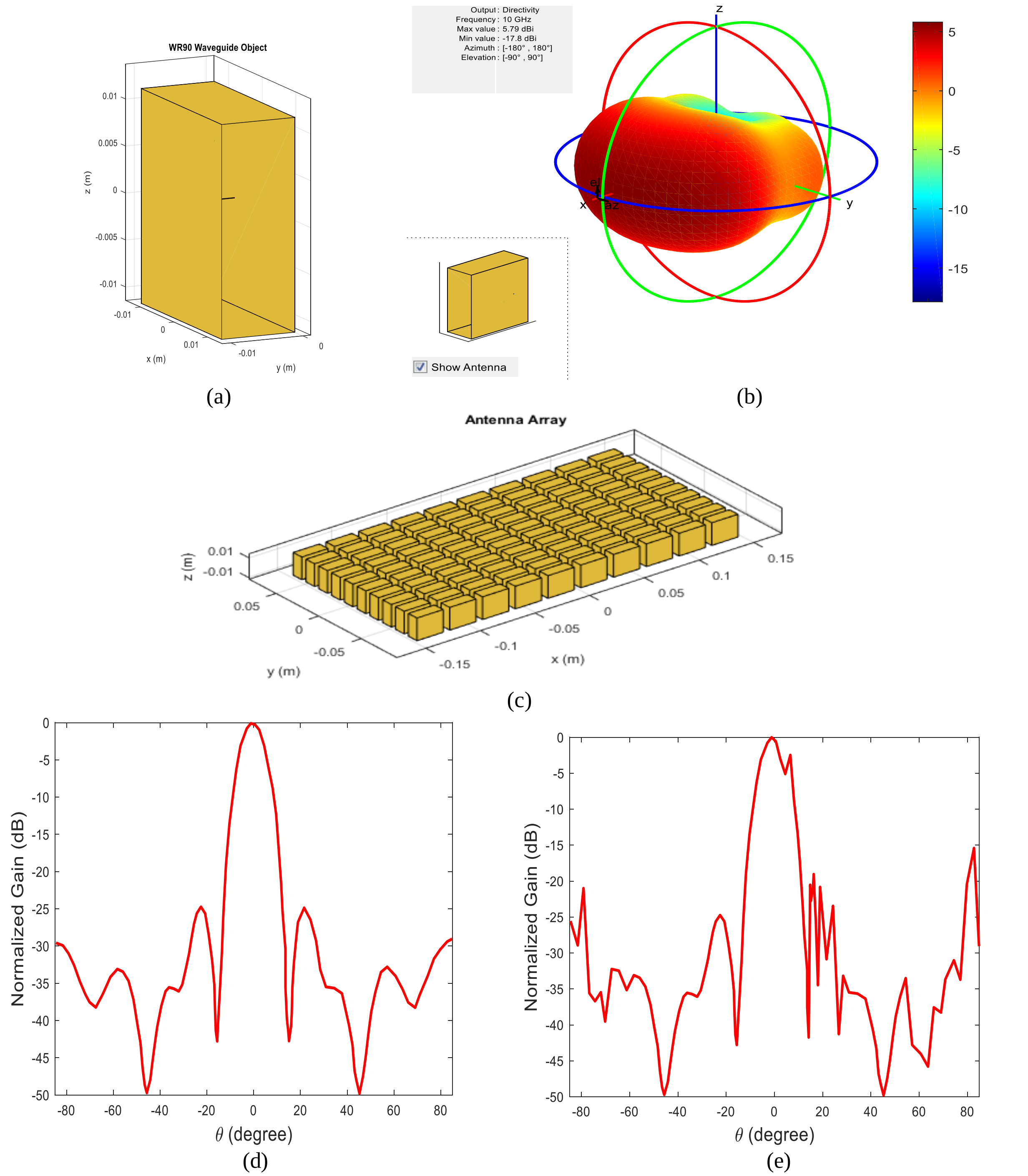

Fig. 2. Simulation setup. (a) Waveguide, (b) radiation pattern, (c) antenna array, (d) normalized radiation pattern with no element failure, and (e) normalized radiation pattern with 6 elements failures.

V. RECOVERY PERFORMANCE

Quantifying the diagnostic performances, the following indicator is introduced. Firstly, we add the field's magnitude samples x_k situated on each element's aperture g: $\alpha_g = \sum_g \left| x_k^g \right|, for\ g = 1, \ldots, G$. From that, we get a positive number for each radiating element g, the difference Δ_{FA} between lowest failure level and highest false alarm is computed. Δ_{FA} value is the margin set as threshold to differentiate between true failure and false alarm. Higher margin Δ_{FA} implies easier diagnostic, while a negative Δ_{FA} implies incorrectly performed diagnostic because false alarm value appears bigger than a failure.

For all the methods adopted, we repeated the simulation for 120 times with the incorporation of the Gaussian white noise. The simulation results given in this study are average figures over the 120 simulation times, so as to ensure appreciable results. The total number of measurement employed for investigation is $12 \times 12 = 144$ for all the methods because choosing higher measured points have no effect on the recovery performance. The associated parameter ϵ in the data-fitting of the sparse recovery techniques (Eqn. 4) is selected to be higher than noise intensity. We specifically put ϵ at $1.1\|\boldsymbol{n}\|_2$ while in measurements, an estimation of the SNR is employed to calculate ϵ. Anechoic chamber that exhibits various SNR is assumed, and we set the value of ϵ accordingly.

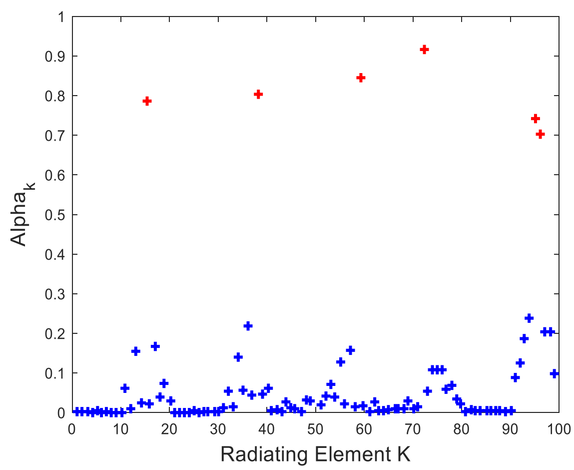

Fig. 3. Result sample of array diagnosis. $alpha_k$ is the radiating element k level. Δ_{FA} is the distance or gap between the least of the six errors (red) and the highest false alarm (black).

D. Amplitude failures

At first we consider *K=6* waveguides are excited with $1 - \delta_A$ amplitude as against 1 to initiate amplitude failures. Accessing the recovery performance, the margin Δ_{FA} is computed for different SNRs. The results are reported in Fig. 3 and Tables 1 and 2 respectively.

It is simpler to conduct diagnosis when amplitude error is more important which is as expected. Generally, for a particular SNR, Δ_{FA} is higher when $\delta_A = 1$ than $\delta_A = 0.1$. The ℓ_1 Norm exhibit highest Δ_{FA} in both cases, this implies best diagnostic performance at different SNRs. Though it took longer simulation time than other compressed sensing methods.

E. Phase failures

In this case, *K=6* waveguides are excited with amplitude of $e^{j\delta_\Phi}$ instead of 1 to emulate failures in phase. Δ_{FA} was computed for different SNRs to evaluate the recovery. The results obtained are shown in Tables 3 and 4. All the comments made for amplitude failures also hold here. As expected, larger phase error is much easier to diagnose than smaller one. The best diagnostic results are obtained by ℓ_1 norm approach.

Generally, the diagnosis is weak at lower SNRs for both amplitude and phase errors. Therefore, this is a gap to be filled up by new algorithms, which is open for research and development. The algorithm should exhibit higher Δ_{FA} recovery performance both at higher and lower SNRs. Because most near-field equipment exhibit different degrees of SNRs, it will make the diagnosis better and correct. But based on this study, ℓ_1 norm offer better diagnosis at lower SNRs; 20 dB and 10 dB from near-field. In all the cases considered for both amplitude and phase failures, and results obtained in Table 1-4, ℓ_1 norm has widest Δ_{FA} gap among the three regularizers considered. Next is TV, which performs better than the mixed l_1/l_2 norm. For instance, at 10 dB SNR of Table 1-4, only ℓ_1 norm gives value for Δ_{FA}. This case is the same for $\delta_A = 1$ and $\delta_A = 0.1$ amplitude failure configurations, and $\delta_\Phi = 70^0$ and $\delta_\Phi = 10^0$ phase failure configurations. Therefore, ℓ_1 norm is the best choice among the three CS methods for all SNR levels considered.

Ensuring common ground for comparison with reference [11], the diagnosing scheme and the AUT configurations are made similar to [11], but the diagnosing results are different. In [11], the mixed l_1/l_2 norm minimization indicates best performance, while in this study; the ℓ_1 norm minimization indicates best performance. The disparity might be because of the nature of field considered. In [11], the CS methods are investigated at far-field, but in this work and that of Migliore [7], minimization $l_1$technique show best performance and more robust against measurement noise. Probably because [7] and this work are investigated at near-field (i.e., measurement is taken on part of hemispherical surface $(0 \leq \theta \leq \pi/2, 0 \leq \phi \leq 2\pi)$ at radius r from center of AUT, and $r < 2D^2/\lambda$. The minimization $l_1$technique does not require any hardware modification of standard (i.e., not scattering-modulated based) near-field measurement systems allowing an increasing of the "throughput" of the array testing process at practically zero cost.

The key point regularization procedure minimizing the 1-norm of the difference vector between a failure-free excitation vector and the excitation vector of the AUT. This allows to obtain an equivalent sparse array, discarding the pieces of information not of interest for the failure identification problem.

This study centers on numerical experiments and shows that the ℓ_1 norm technique gives best performance. However, the identification of the minimum number of measurements in array diagnosis, and in general the development of precise undersampling theorems in electromagnetic theory, remains an open problem that requires further studies.

Table 1: Recovery performance for various *SNR*s; *K=6* amplitude failures and $\delta_A = 1$ amplitude failure configuration

SNR (dB)	100	80	60	40	20	10
Δ_{FA} of L_1L_2	0.4251	0.3997	0.3196	0.1982	NAN	NAN
Δ_{FA} of TV	0.9846	0.8636	0.6738	0.6321	0.3121	NAN
Δ_{FA} of L_1	0.9997	0.9892	0.9771	0.8562	0.4321	0.021

Table 2: Recovery performance for various *SNR*s; *K=6* amplitude failures and $\delta_A = 0.1$ amplitude failure configuration

SNR (dB)	100	80	60	40	20	10
Δ_{FA} of L_1L_2	0.4531	0.2310	0.0000	NAN	NAN	NAN
Δ_{FA} of *TV*	0.5312	0.3921	0.2101	0.1031	0.0010	NAN
Δ_{FA} of L_1	0.8251	0.7834	0.7321	0.6101	0.3221	0.0310

Table 3: Recovery performance for various *SNR*s; *K=6* phase failures and $\delta_\Phi = 70^0$ phase failure configuration

SNR (dB)	100	80	60	40	20	10
Δ_{FA} of L_1L_2	0.7984	0.7231	0.6321	0.1321	NAN	NAN
Δ_{FA} of TV	0.5312	0.3921	0.4210	0.4521	0.0210	NAN
Δ_{FA} of L_1	0.9876	0.9231	0.8532	0.6324	0.3871	0.1310

Table 4: Recovery performance for various *SNR*s; *K=6* phase failures and $\delta_\Phi = 10^0$ phase failure configuration

SNR (dB)	100	80	60	40	20	10
Δ_{FA} of L_1L_2	0.4421	0.3410	0.3750	NAN	NAN	NAN
Δ_{FA} of *TV*	0.6120	0.5881	0.5101	0.0000	NAN	NAN
Δ_{FA} of L_1	0.8612	0.7994	0.7821	0.2101	NAN	NAN

VI. CONCLUSION

In this paper, a recovery performance analysis test of compressive sensing methods for antenna array diagnosis from near-field measured data is presented. Particularly, we considered three prominent regularization procedures: total variation (TV), mixed l_1/l_2 norm, and minimization of the l_1 to solve diagnosis problems in antenna array at low SNR. Simulation of a 10 GHz 10×10 rectangular waveguide array under realistic noise conditions was presented and used to conduct the test for various SNRs. Generally, the diagnosis is weak at low SNRs for both amplitude and phase errors, so for data with low SNRs. Minimization l_1 technique show more robustness to additive data noise than total variation, and mixed l_1/l_2 norm. Therefore, minimization l_1 is a better choice whenever antenna array diagnosis is to be performed in a very harsh measurement environment.

ACKNOWLEDGMENT

This work is supported in part by Global Excellence Stature (GES) of the University of Johannesburg, South Africa.

REFERENCES

[1] J. A. Rodriguez, F. Ares, E. Moreno, and G. Franceschetti, “Genetic algorithm procedure for linear array failure correction,” *Electron. Lett.*, vol. 36, no. 3, pp. 196-198, Feb. 2000.

[2] R. Iglesias, F. Ares, M. Fernandez-Delgado, J. A. Rodriguez, J. Bregains, and S. Barro, “Element failure detection in linear antenna arrays using case-based reasoning,” *IEEE Antennas Propag. Mag.*, vol. 50, no. 4, pp. 198-204, Aug. 2008.

[3] O. M. Bucci, M. D. Migliore, G. Panariello, and P. Sgambato, “Accurate diagnosis of conformal arrays from near-field data using the matrix method,” *IEEE Trans. Antennas Propag.*, vol. 53, no. 3, pp. 1114-1120, Mar. 2005.

[4] J. A. Rodriguez-Gonzalez, F. Ares-Pena, M. Fernandez-Delgado, R. Iglesias, and S. Barro, “Rapid method for finding faulty elements in antenna arrays using far field pattern samples,” *IEEE Trans. Antennas Propag.*, vol. 57, no. 6, pp. 1679-1683, June 2009.

[5] A. Buonanno, and M. D’Urso, “On the diagnosis of arbitrary geometry fully active arrays,” *in Proc. Eur. Conf. Antennas Propag.* (EuCAP), Barcelona, Spain, pp. 1-4.S, Apr. 2010.

[6] S. Clauzier, S. M. Mikki, and Y. M. M. Antar, “Design of near-field synthesis arrays through global optimization,” *IEEE Trans. Antennas Propag.*, vol. 63, no. 1, pp. 151-165, Jan. 2015.

[7] M. D. Migliore, "A compressed sensing approach for array diagnosis from a small set of near-field measurements," *IEEE Trans. Antennas Propag.*, vol. 59, no. 6, pp. 2127-2133, June 2011.

[8] G. Oliveri, P. Rocca, and A. Massa, "Reliable diagnosis of large linear arrays—A Bayesian compressive sensing approach," *IEEE Trans. Antennas Propag.*, vol. 60, no. 10, pp. 4627-4636, Oct. 2012.

[9] O. Famoriji, Z. Zhang, A. Fadamiro, R. Zakariyya, and F. Lin, "Planar array diagnostic tool for millimeter-wave wireless communication systems," *Electronics*, vol. 7, no. 383, 2018.

[10] O. J. Famoriji, Z. Zhang, A. Fadamiro, Z. Khan, and F. Lin, "Active antenna array diagnosis from far-field measurements," *IEEE Int. Conference on Integrated Circuits, Technologies and Applications* (ICTA), Beijing, China, pp. 1-2.S, Dec. 2018.

[11] B. Fuchs, L. L. Coq, and M. D. Migliore, "Fast antenna array diagnosis from a small number of far-field measurements," *IEEE Trans. Antennas Propag.*, vol. 64, no. 6, pp. 2227-2235, June 2016.

[12] A. F. Morabito, R. Palmeri, and T. Isernia, "A compressive-sensing-inspired procedure for array antenna diagnostic by a small number of phaseless measurements," *IEEE Trans. Antennas Propag.*, vol. 64, no. 7, pp. 3260-3265, July 2016.

[13] 5G: A technological Vision, HUAWEI white paper, Huawei Technologies Co., Shenzhen [Online] Available: http://www.huawei. com/5gwhitepaper/

[14] J. J. Lee, E. M. Ferrer, D. P. Woollen, and K. M. Lee, "Near-field probe used as a diagnostic tool to locate defective elements in an array antenna," *IEEE Trans. Antennas Propag*., vol. 36, no. 3, pp. 884-889, June 1988.

[15] L. Gattoufi, D. Picard, Y. R. Samii, and J. C. Bolomey, "Matrix method for near-field diagnostic techniques of phased array antennas," *in Proc. IEEE Int. Symp. Phased Array Syst. Technol*., pp. 52-57, 1996.

[16] C. Xiong, G. Xiao, Y. Hou, and M. Hameed, "A compressive sensing-based element failure diagnosis method for phased array antenna during beam steering," *IEEE Trans. Antennas Wireless Propag. Lett.*, vol. 18, pp. 1756-1760, Sept. 2019.

[17] M. D. Migliore, "A compressed sensing approach for array diagnosis from a small set of near-field measurements," *IEEE Trans. Antennas Propag.*, vol. 59, no. 6, pp. 2127-2133, June 2011.

[18] G. Oliveri, P. Rocca, and A. Massa, "Reliable diagnosis of large linear arrays, a Bayesian compressive sensing approach," *IEEE Trans. Antennas Propag.*, vol. 60 no. 10, pp. 4627-4636, Oct. 2012.

[19] M. D. Migliore, "Array diagnosis from far-field data using the theory of random partial Fourier matrices," *IEEE Trans. Antennas Wireless Propag. Lett.*, vol. 12, pp. 745-748, July 2013.

[20] B. Fuchs and M. D. Migliore, "Accurate array diagnosis from near-field measurements using reweighted minimization," *IEEE Antennas Propag. Symp*., Orlando, FL, USA, pp. 2255-2256, 2013.

[21] B. Fuchs, L. Le Coq, L. Ferro-Famil, and M. D. Migliore, "Comparison of methods for reflectarray diagnostic from far field measurements," *in Proc. IEEE Int. Symp. Antennas Propag*., pp. 398-399, July 2015.

[22] D. L. Donoho, "Compressive sensing," *IEEE Trans. Inf. Theory*, vol. 52, no. 4, pp. 1289-1306, Apr. 2006.

[23] E. J. Candes, J. Romberg, and T. Tao "Robust uncertainty principles: Exact signal reconstruction from highly incomplete frequency information," *IEEE Trans. Inf. Theory*, vol. 52, no. 2, pp. 489-509, Feb. 2006.

[24] D. L. Donoho and J. Tanner, "Precise undersampling theorems," *Proc. IEEE*, vol. 98, no. 6, pp. 913-923, June 2010.

[25] M. D. Migliore, B. Fuchs, L. Le Coq, and L. Ferro-Famil, "Compressed sensing approach for reflectarray diagnostic from far field measurements," *in Proc. Eur. Microw. Conf.*, Sep. pp. 289-292, 2015.

[26] A. Massa, P. Rocca, and G. Oliveri, "Compressive sensing in electromagnetics—A review," *IEEE Antennas Propag. Mag.*, vol. 57, no. 1, pp. 224-238, Feb. 2015.